European Journal of Cell Biology 96 (2017) 705–714

Contents lists available at ScienceDirect

European Journal of Cell Biology

journal homepage: www.elsevier.com/locate/ejcb

Research paper

VAMP8-mediated NOX2 recruitment to endosomes is necessary for antigen release

Ilse Dingjan[a], Laurent M. Paardekooper[a], Daniëlle R.J. Verboogen[a], Gabriele Fischer von Mollard[b], Martin ter Beest[a], Geert van den Bogaart[a,*]

[a] Department of Tumor Immunology, Radboud Institute for Molecular Life Sciences, Radboud University Medical Center, Nijmegen, 6525 GA, The Netherlands
[b] Department of Chemistry, Bielefeld University, Bielefeld, 33501, Germany

ARTICLE INFO

Article history:
Received 13 March 2017
Received in revised form 21 June 2017
Accepted 21 June 2017

Keywords:
Dendritic cells
VAMP8
NOX2
Cross-presentation
Lipid peroxidation

ABSTRACT

Cross-presentation of foreign antigen in major histocompatibility complex (MHC) class I by dendritic cells (DCs) requires activation of the NADPH-oxidase NOX2 complex. We recently showed that NOX2 is recruited to phagosomes by the SNARE protein VAMP8 where NOX2-produced reactive oxygen species (ROS) cause lipid oxidation and membrane disruption, promoting antigen translocation into the cytosol for cross-presentation. In this study, we extend these findings by showing that VAMP8 is also involved in NOX2 trafficking to endosomes. Moreover, we demonstrate in both human and mouse DCs that absence of VAMP8 leads to decreased ROS production, lipid peroxidation and antigen translocation, and that this impairs cross-presentation. In contrast, knockdown of VAMP8 did not affect recruitment of MHC class I and the transporter associated with antigen processing 1 (TAP1) to phagosomes, although surface levels of MHC class I were reduced. Thus, in addition to a secretory role, VAMP8-mediates trafficking of NOX2 to endosomes and phagosomes and this promotes induction of cytolytic T cell immune responses.

1. Introduction

Dendritic cells (DCs) are key antigen presenting cells of the immune system that take up pathogens by endocytosis and phagocytosis to kill, degrade and finally present pathogen-derived antigens for activation of T cells (Cruz et al., 2017; Joffre et al., 2012; Nair-Gupta and Blander, 2013). Activation of CD8+ 'killer' T cells requires ingested antigens to be presented on major histocompatibility (MHC) class I molecules following a process called cross-presentation. Essential for cross-presentation is the NADPH oxidase NOX2 complex which resides on endosomes and phagosomes, and produces reactive oxygen species (ROS) within the endo/phagosomal lumen (Dingjan et al., 2016; Jancic et al., 2007; Kotsias et al., 2013; Mantegazza et al., 2008; Nunes et al., 2013; Savina et al., 2006). NOX2 promotes antigen cross-presentation by three mechanisms. First, ROS production results in alkalization of the endosomal lumen, thereby inhibiting activation of lysosomal proteases with low pH optima and preventing excessive antigen degradation (Jancic et al., 2007; Kotsias et al., 2013; Savina et al., 2006). Second, lysosomal proteases of the cystein cathepsin family are reversibly oxidized by ROS, which also preserves antigen (Allan et al., 2014; Hari et al., 2015; Rybicka et al., 2012). Last, we showed that NOX2-produced ROS oxidize lipids of the endosomal membrane, resulting in membrane disruption and release of antigen from the endosomal lumen into the cytosol (Dingjan et al., 2016). Within the cytosol, the antigen becomes accessible to proteasomal degradation for generation of MHC class I-compatible peptides (Cruz et al., 2017; Joffre et al., 2012; Nair-Gupta and Blander, 2013).

Recently, we examined how the integral membrane component of NOX2, cytochrome b_{558}, which consists of gp91^{phox} and p22^{phox}, traffics to antigen-containing phagosomes in human blood-isolated monocyte-derived DCs (Dingjan et al., 2017). We showed that gp91^{phox} is recruited from the plasma membrane to phagosomes during their formation. After, or perhaps already during, phagosome sealing, phagosomal NOX2 is replaced from intracellular compartments of late endosomal/lysosomal nature and this serves to replace oxidatively damaged NOX2. The final fusion step that merges NOX2-containing transport vesicles with the phagosomal membrane is catalyzed by the complexing of the SNARE proteins VAMP8 with syntaxin-7 and SNAP23 (Dingjan et al., 2017). In mouse DCs, this trafficking step is targeted by the intracellular pathogen *Leishmania*, which selectively cleaves VAMP8 thereby preventing

* Corresponding author at: Radboud University Medical Center, Geert Grooteplein 26–28, 6525 GA, Nijmegen, The Netherlands.
E-mail address: geert.vandenbogaart@radboudumc.nl (G. van den Bogaart).

http://dx.doi.org/10.1016/j.ejcb.2017.06.007

NOX2 function and cross-presentation and evading immune recognition (Matheoud et al., 2013).

In this study, we sought to determine whether VAMP8 would also be responsible for trafficking of NOX2 components to endosomes and whether this would be important for antigen cross-presentation by human DCs. Our data show that siRNA knock-down of VAMP8 resulted in impaired recruitment of gp91^{phox}, but not of MHC class I and the transporter associated with antigen processing 1 (TAP1), to endosomes and phagosomes in human blood-derived DCs, corroborating our previous findings (Dingjan et al., 2017). Moreover, we show that the lack of VAMP8 leads to reduced formation of endosomal ROS and decreased oxidation of endosomal components, which in turn blocked the translocation of antigen into the cytosol. VAMP8 knockdown impaired antigen cross-presentation by human DCs, similar to previous findings with VAMP8-negative mouse DCs (Matheoud et al., 2013). Finally, our data indicate that VAMP8 is involved in multiple transport routes within DCs, and, in addition to the recruitment of NOX2 to the antigen-containing compartment, mediates trafficking of MHC class I to the plasma membrane. Our study strengthens the emerging concept that the replenishment of NOX2 from late endosomal/lysosomal compartments is important for antigen cross-presentation and the initiation of cytolytic T cell immune responses.

2. Material and methods

2.1. Cell culture

Human DCs were derived from peripheral blood mononuclear cells (PBMCs) obtained from healthy volunteers according to institutional guidelines and as described previously (Dingjan et al., 2016). Briefly, monocytes were differentiated into immature DCs by culturing for 6 days at 37 °C, 5% CO_2 in the presence of 300 U/ml interleukin-4 and 450 U/ml GM-CSF in complete RPMI-1640 (containing 10% fetal bovine serum (FBS), 2 mM UltraGlutamine and 1% Antibiotic-Antimytotic (AA)). Jurkat E6.1 cells were used for the T cell activation assays with human DCs. These cells contain CD8+ T cell receptors that recognize gp100-peptide (residues 280–288) in complex with HLA-A2. They were cultured in the presence of 5 ng/ml interleukin-2 in complete RPMI-1640. Mouse bone marrow derived DCs (BMDCs) from VAMP8-/- mice (JAX strain B6;129S-Vamp8$^{Gt(OST20346)Lex}$/J) were differentiated by culturing 7 days in the presence of 20 ng/ml GM-CSF in RPMI-1640 containing 10% FBS, 2 mM UltraGlutamine, 1% AA and 28 μM b-mercaptoethanol.

2.2. siRNA knock-down

DCs were electroporated with siRNA against VAMP8 (mix of 3 siRNAs: 5′-GAGGA AAUGA UCGUG UGCGG AACCU-3′, 5′-GAGGU GGAGG GAGUU AAGAA UAUUA-3′, 5′-CGACA UCGCA GAAGG UGGCU CGAAA-3′; ThermoFisher) or with non-targeting stealth RNAi siRNA Negative Control (NT) siRNA#1 (ThermoFisher) using a Neon Transfection System (ThermoFisher; 1000 V, 40 ms, 2 pulses) as described (Baranov et al., 2016; Dingjan et al., 2017, 2016). Cells were used 48 h post-transfection to ensure maximal knock-down. To test knock-down efficiency, DCs were lysed with 1% SDS in 10 mM Tris-HCl at pH 6.8 and lysates (20 μg total protein) were ran on 16% Tricine-SDS-PAGE and blotted to PVDF. VAMP8 was detected with rabbit anti-serum raised against VAMP8 (1:1000 dilution; catalog nr. 104 302, Synaptic Systems) in combination with goat anti-rabbit conjugated with IRDye 800 (Li-Cor) as secondary antibody (1:5000).

2.3. Plasmid transfection

DCs were transfected with 8 μg of a plasmid encoding human Rab11a N-terminally fused to GFP (Choudhury et al., 2002) per 1×10^6 cells using a Neon Transfection System (ThermoFisher; 1000 V, 40 ms, 2 pulses) as described (Baranov et al., 2014). Cells were stimulated with zymosan particles 4 h post-transfection, followed by immunostaining with anti-gp91^{phox}.

2.4. Antigen uptake

Uptake of bovine serum albumin (BSA) labeled with Alexa fluor 488 was measured by incubating DCs with 100 μg/ml BSA-Alexa Fluor 488 (ThermoFisher) and 1 μg/ml LPS (Invivogen, catalog number TLR-eblps; isolated from *Escherichia coli* 0111:B4, UltraPure) for different time points. After incubation, the cells were washed and the percentage of BSA-AF488 positive cells was measured by flow cytometry (excitation: 488 nm; emission: 530/30 nm; FACS Caliber, BD biosciences).

2.5. Immunofluorescence

Cells were cultured at 50,000 cells per 12 mm diameter coverslip in the presence of 4.5 μm-sized microspheres (10 beads/cell; Polysciences), ovalbumin conjugated with Alexa Fluor 647 (2.5 μg/ml; OVA; Hyglos, catalog number 321000; endotoxin-free) or Alexa Fluor 633-labelled zymosan particles (5 particles/cell) in serum-free RPMI for 1 h at 37 °C. Cells were fixed with 4% PFA for 15 min and permeabilized and blocked with 0.1% saponin in CLSM-buffer (PBS with 20 mM glycine and 3% BSA) at room temperature. For immunostaining, cells were incubated overnight at 4 °C with rabbit serum anti-VAMP8 (104302, Synaptic Systems), mouse-IgG1 anti-gp91^{phox} (D162-3, MBL), mouse-IgG1 anti-TAP1 (MABF125, Millipore), mouse-IgG2a anti-HLA class I (ab7855, Abcam), mouse-IgG2a anti-SEC22 B (sc-101267, Santa Cruz), mouse-IgG1 anti-ERGIC-53 (ABS300, Enzo) and/or rabbit serum anti-Calnexin (ab22595, Abcam) at 1:200 dilution in CLSM-buffer containing 0.1% saponin. Subsequently, the cells were washed and incubated with goat anti-rabbit IgG labeled with Alexa Fluor 568 or 647 and goat anti-mouse IgG labeled with Alexa Fluor 488 (both Life Technologies) as secondary antibodies at 1:400 dilution. Finally, the cells were washed and embedded in mounting medium containing 0.01% Trolox (6-hydroxy-2,5,7,8-tetramethylchroman-2-carboxylic acid) and 68% glycerol in 200 mM sodium phosphate buffer at pH 7.5. Cells were imaged on an Olympus FV1000 confocal laser scanning microscope with a 60 × 1.35 NA oil immersion objective.

2.6. DC phenotyping

Cells were incubated overnight with or without 1 μg/ml LPS, detached and blocked with human serum. This was followed by surface staining for 30 min at 4 °C with the following antibodies for human DCs (all BD Biosciences): PE-labeled anti-HLA-A2 (catalog number 558570), anti-HLA-DR (555812), anti-CD11c (333149) and anti-CD86 (555658), APC-labeled anti-CD86 (555660) and FITC-labeled anti-CD83 (556910). The following antibodies were used for mouse DCs: PE-labeled anti-HLA-A2 (114608; Biolegend), anti-HLA-DR (12-5321-82; eBioscience), anti-CD11c (553802; BD Biosciences) and anti-CD86 (105008; Biolegend). After washing, fluorescence intensities were measured by flow cytometry (FACS Caliber).

Cytokines levels in supernatants of human DCs transfected with NT or VAMP8 siRNA was assessed with the Proteome Profiler Human Cytokine Array Kit (ARY005; R&D systems) following the protocol of the manufacturer, except that the membrane was

stained with IRDye 800CW Streptavidin and imaged with the Odyssey CLx Infrared Imaging System (Li-Cor).

2.7. ROS measurements

To measure cellular production of H_2O_2, we used the Amplex Red assay as described previously (Dingjan et al., 2016). Briefly, cells were incubated for 2–4 h in a 96 well plate (100,000 cells/well) in serum-free RPMI with 2.2 μM OVA (Hyglos, endotoxin-free) and 1 μg/ml LPS (Invivogen, *E. coli* 0111:B4). This is UltraPure LPS without contaminants of other bacterial components that can influence cross-presentation (Wagner and Cresswell, 2012). After incubation, the medium was changed for serum-free RPMI containing 50 μM Amplex UltraRed reagent (ThermoFisher) and 3 U/ml horseradish peroxidase (Sigma) and the fluorescence of resorufin (excitation: 530 nm; emission: 590/30 nm) was measured every 20 min during 2 h of subsequent incubation.

Production of superoxide anion was measured with 2′,7′-dichlorodihydrofluorescein diacetate (H_2DCFDA) (ThermoFisher). Briefly, DCs were washed once with cold PBS, followed by incubation on ice for 30 min with zymosan particles (5 particles/cell). After this pulse, the pulse-chase samples were washed 3 times with cold PBS. Then H_2DCFDA was added at a concentration of 10 μg/ml to each sample and fluorescence (excitation: 485/20 nm; emission: 530/30 nm) was measured after different incubation times using a CytoFluor II microplate reader (ThermoFisher). Background fluorescence was subtracted and samples were normalized to the amounts of cells as determined by the 3-(4,5-dimethylthiazol-2-yl)-2,5-diphenyltetrazolium bromide (MTT) assay.

Lipid peroxidation was measured with the BODIPY581/591-C11 assay as described previously (Dingjan et al., 2016). DCs were loaded with 2.2 μM OVA, 1 μg/ml LPS and cultured in the presence of 1 μM BODIPY581/591-C11 (4,4-difluoro-5-(4-phenyl-1,3-butadienyl)-4-bora-3a,4a-diaza-s-indacene-3-undecanoic acid; ThermoFisher) in serum-free RPMI for different time points at room temperature. After incubation, the BODIPY581/591-C11 fluorescence was measured by flow cytometry (excitation: 488 nm; emission: 530/30 nm; FACS Caliber). The signal from unstained cells was subtracted for background correction.

2.8. CCF4/β-lactamase assay

The CCF4/β-lactamase assay was performed in Willco petri dishes according to the protocol of the manufacturer (K1095, Life Technologies) and as described previously (Dingjan et al., 2016). Briefly, DCs were incubated with 1 μM Substrate Loading Solution and 1 μg/ml LPS as adjuvant for 90 min, then washed and incubated with 1 mg/ml β-lactamase (from *Pseudomonas aeruginosa*, expressed in *E. coli*; L6170, Sigma) and 1 μg/ml LPS for 3 h. Cells were washed again and imaged with a Leica SP8 confocal microscope equipped with a 63 × 1.20 NA water immersion objective (405 nm excitation; 419–458 nm blue and 504–600 nm green emission of the coumarin donor and fluorescein acceptor fluorophores, respectively). The FRET cleavage was calculated as the ratio of the green over the blue fluorescence intensities. The FRET efficiency of cells in absence of β-lactamase was used as 'no cleavage' control.

2.9. Cross-presentation assay

For the T cell activation assay, HLA-A2 positive human DCs were adhered for 1 h at 37 °C in X-vivo medium (Lonza) containing 2% human serum in 96 wells plates. Cells were then washed and incubated with gp100 short (10 μM gp100 (residues 280–288); GenScript) or long (100 μM gp100 (residues 272–300); JPT) peptide with T cell receptor stimulation mix (4 μg/ml R-848 and poly(I:C); Enzo Life Sciences) for 4 h. After incubation, cells were washed and resuspended in X-vivo medium containing Jurkat E6.1 cells (ratio 1 DC: 2 T cells) and co-cultured for 18 h at 37 °C. T cells were stained with αCD69-FITC (1:10; BD biosciences), αCD3-APC (1:10; eBiosciences) and Propidium Iodide (PI; 0.5 μg/ml) and analyzed with a FACS Calibur (BD biosciences). CD69 surface levels as a measure of T cell activation were analyzed using FlowJo software and Prism 5. Briefly, cells were gated on viability (PI), followed by gating for CD3-positive cells, and the CD69 signals were determined. T cell activation was calculated as the ratio of CD69 positive cells stimulated with long over stimulation with short peptide.

2.10. Statistical analysis

Results of at least three independent experiments were plotted as raw data or normalized to control cells (100%). All experiments were assessed using paired Student's *t*-tests or two-way ANOVA (following post-hoc Bonferroni's test). Two-sided P values <0.05 were considered to be statistically significant ($^{*}p < 0.05$, $^{**}p < 0.01$, $^{***}p < 0.001$).

3. Results

To investigate the role of VAMP8 in antigen cross-presentation in human DCs, we performed siRNA knockdown of VAMP8 in blood-isolated monocyte-derived DCs. We achieved 79 ± 11% (average ± S.D. from 9 different donors) knockdown efficiency by Western blot (Fig. 1A). We also generated bone marrow derived DCs (BMDCs) from VAMP8-/- mice. VAMP8 is a SNARE protein that catalyzes various endosomal and secretory membrane fusion steps and locates to both early and late endosomes as well as to phagosomes and secretory vesicles (Antonin et al., 2000; Dressel et al., 2010; Ho et al., 2008; Nagamatsu et al., 2001; Paumet et al., 2000; Polgár et al., 2002; Pryor et al., 2004). VAMP8 also has a secretory function in DCs as VAMP8 ablation led to a significant reduction of the surface levels of MHC class I in human DCs and of both MHC class I and II in mouse DCs (Fig. 1B–C). Moreover, VAMP8 knockdown resulted in a trend of reduced secretion of interleukin-1 receptor antagonist (IL-1ra; Fig. 1D–E). These results indicate that VAMP8 could mediate the exocytosis of secretory vesicles containing MHC molecules and IL-1ra and/or plays a role at upstream trafficking events.

Recently, we showed that VAMP8 mediates the recruitment of $gp91^{phox}$ to zymosan-containing phagosomes in human DCs (Dingjan et al., 2017). Others (Matheoud et al., 2013) showed that VAMP8 also mediates recruitment of $gp91^{phox}$ to latex beads and *Leishmania*-containing phagosomes in mouse DCs. In line with this, we observed that siRNA knockdown of VAMP8 resulted in a reduction of $gp91^{phox}$ recruitment to both latex-bead bearing phagosomes and OVA-containing endosomes compared to the non-targeting siRNA control (Fig. 2A–B). Thus, our data show that VAMP8 mediates the recruitment of $gp91^{phox}$, the integral membrane component of NOX2, to antigen-containing endosomes and phagosomes in human DCs, corroborating previous findings in human and mouse DCs (Dingjan et al., 2017; Matheoud et al., 2013). Importantly, VAMP8-mediated recruitment of $gp91^{phox}$ seems to be a general mechanism that does not depend on signaling by pathogen recognition receptors (PRR), as it was observed for a wide range of model antigens and also for latex beads that do not activate PRRs (Fig. 2A–B; Dingjan et al., 2017; Matheoud et al., 2013).

We then tested whether the reduced phagosomal recruitment of $gp91^{phox}$ upon VAMP8 knockdown would lead to impaired cellular ROS production. VAMP8-knockdown DCs produced less H_2O_2 compared to non-targeting siRNA control cells, as measured with the Amplex Red assay (Fig. 2C). In these experiments, we stimulated the DCs with the Toll like receptor 4 (TLR4) agonist lipopolysaccharide

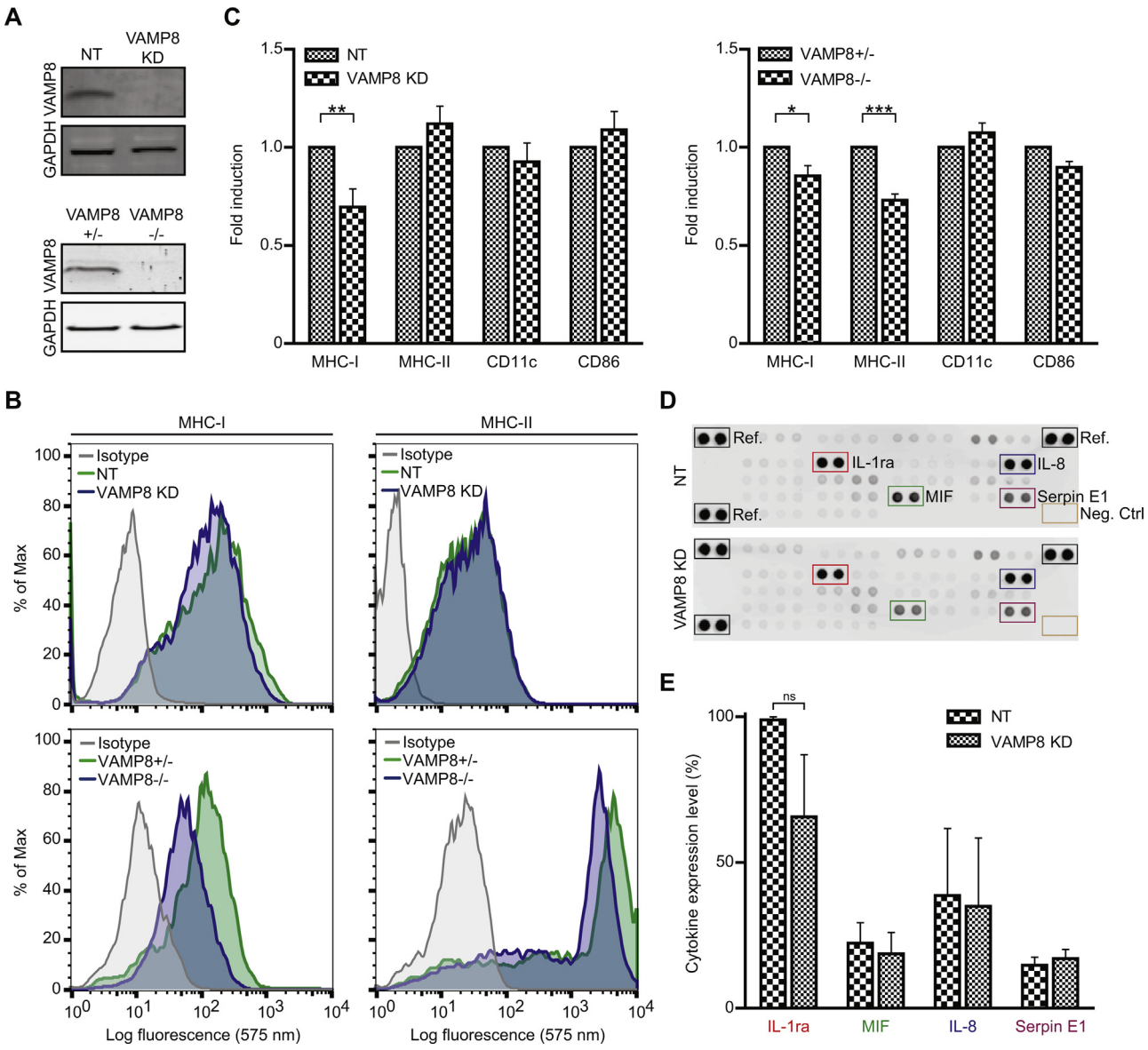

Fig. 1. Loss of VAMP8 results in decreased surface-levels of MHC class I. (A) siRNA knockdown for VAMP8 in human DCs (VAMP8 KD; NT: non-targeting siRNA; see reference (Dingjan et al., 2016) for quantification) and VAMP8 expression in BMDCs from VAMP8± and −/− mice by Western blot. GAPDH: loading control. (B) Representative flow cytometry histograms of surface staining of MHC class I and II molecules in VAMP8 KD (blue) and NT (green) human DCs (upper graphs) and for VAMP8−/− (blue) and VAMP8± (green) mouse BMDCs (lower graphs). The grey curves show the mean fluorescence intensities of the isotype controls. (C) Expression levels of HLA-A2 molecules (MHC-I), HLA-DR molecules (MHC-II), CD11c or CD86 on the surface of VAMP8 KD human DCs (left) or VAMP8-/- mouse BMDCs (right) normalized to control cells. (D) Representative dot blot cytokine array blots for NT and VAMP8 KD human DCs. The grey values are proportional to the levels of secreted cytokines. The 4 most abundant cytokines are indicated: IL-1ra; macrophage migration inhibitory factor (MIF); interleukin-8 (IL-8); Serpin E1. (E) Quantification of the cytokine secretion levels from panel D normalized to the highest intensities. Results are from at least three donors and plotted as mean ± s.e.m. (For interpretation of the references to colour in this figure legend, the reader is referred to the web version of this article.)

(LPS) O111:B4 from *E. coli* which results in increased surface levels of the maturation markers MHC class I, MHC class II, CD86 and CD83 (Sup. Fig. 1), and is known to promote the cross-presentation efficiency of DCs (Wagner and Cresswell, 2012). For our ROS measurements, it did not matter whether the antigen was continuously present with the DCs or washed away after initial preincubation at 4 °C (where the antigen binds but is not taken up; Sup. Fig. 2A). Previously, VAMP8 was shown to act as a negative regulator of phagocytosis, because VAMP8-negative mouse DCs showed an increased phagocytosis while VAMP8 overexpression resulted in the reverse effect (Ho et al., 2009, 2008). However, for our human monocyte-derived DCs, we did not observe an effect of VAMP8 on phagocytosis and VAMP8-knockdown DCs ingested zymosan or latex particles with similar efficiency as control cells. Endocytosis was also not affected by VAMP8, as the uptake of the model antigen albumin from bovine serum (BSA) labeled with Alexa Fluor 488 by VAMP8-knockdown DCs was not changed (Sup. Fig. 2B–C). Thus, we did not observe effects of VAMP8 knockdown on antigen uptake, indicating that the decreased cellular ROS production in absence of VAMP8 is likely caused by the impaired trafficking of NOX2 to the antigen-containing compartment.

ROS react indiscriminately and hence NOX2 activity causes self-damage by oxidizing endosomal and phagosomal proteins and lipids within the DC (Allan et al., 2014; Dingjan et al., 2017, 2016; Hari et al., 2015; Rybicka et al., 2012). We expected that the absence of VAMP8 would reduce this damage, since our results show that siRNA knockdown of VAMP8 results in impaired endosomal and phagosomal recruitment of gp91^{phox} and reduced ROS produc-

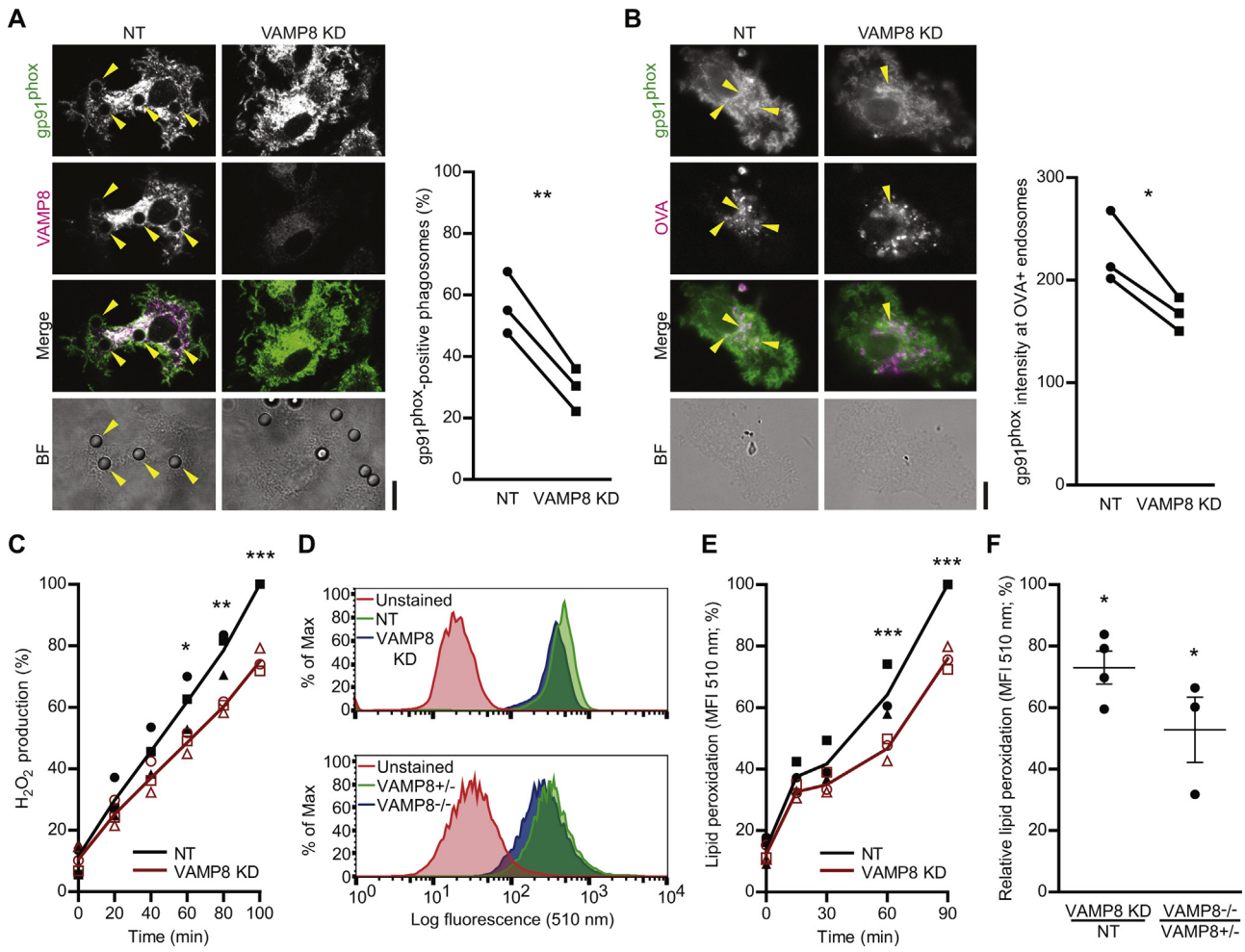

Fig. 2. VAMP8 is responsible for NOX2 recruitment to endosomes and phagosomes. (A) Representative confocal micrographs showing the recruitment of gp91^{phox} (green in merge) to phagosomes containing latex beads by immunofluorescence in VAMP8 KD DCs and control DCs (non-targeting siRNA; NT). Magenta: immunolabeling for VAMP8. Arrow heads indicate phagosomes positive for gp91^{phox}. The graph shows the quantification by manual counting of gp91^{phox}-positive phagosomes of DCs from 3 individual donors (linked by solid lines; p = 0.0067). (B) Same as panel A, but now for ovalbumin-containing endosomes (OVA; magenta; p = 0.0391). Recruitment was quantified from the gp91^{phox} signal at OVA-positive compartments relative to the total imaged cell area. (C) H_2O_2 production by VAMP8 KD DCs (red curve) compared to NT control DCs (black) measured with the Amplex Red assay. The symbols show the individual donors. (D) Representative flow cytometry histograms of lipid peroxidation sensor BODIPY581/591-C11 for VAMP8 KD (blue) and NT (green) human DCs (upper graph) and for VAMP8−/− (blue) and VAMP8± (green) mouse BMDCs (lower graph) after 60 min incubation with LPS and OVA. The red curves show the background fluorescence distribution from cells without BODIPY581/591-C11. (E) Percentage of lipid peroxidation over time in VAMP8 KD (red curve) and NT (black) human DCs. The symbols show the individual donors. (F) Quantification of panel D. Relative lipid peroxidation: mean fluorescence intensities of VAMP8 KD DCs (4 donors; p = 0.0154) and VAMP8-/- BMDCs (3 mice; p = 0.0474) relative to the NT and VAMP8± controls. Scale bars, 10 μm. (For interpretation of the references to colour in this figure legend, the reader is referred to the web version of this article.)

tion. To investigate this possibility, we measured peroxidation of cellular lipids with the lipid peroxidation probe BODIPY581/591-C11 in human DCs. This probe mimics a poly-unsaturated lipid and its oxidation results in an increased fluorescence emission at 510 nm that can be measured by flow cytometry (Fig. 2D). Incubating human DCs with this probe revealed time-dependent lipid peroxidation, and this was reduced in DCs with siRNA knockdown of VAMP8 compared to DCs transfected with non-targeting siRNA (Fig. 2E). This reduction in lipid peroxidation was similar to what we observed previously with siRNA knockdown of gp91^{phox}, or upon treatment of the DCs with the NOX2-inhibitor phenylarsine oxide or the lipophilic radical scavenger α-tocopherol (Dingjan et al., 2016). Lipid peroxidation was also reduced in BMDCs isolated from VAMP8-/- mice compared to BMDCs from wild-type mice (Fig. 2F; Kanwar et al., 2008; Matheoud et al., 2013), although in this case LPS maturation only resulted in increased surface expression of CD86 and did not affect MHC class I, MHC class II and CD11c levels (Sup. Fig. 1B). These data show that genetic ablation of VAMP8 results in a significant reduction of lipid peroxidation in both human and mouse DCs (Fig. 2E–F), further supporting the requirement of VAMP8 for NOX2 activity.

We recently showed that the oxidation of endosomal lipids promotes the translocation of antigen from the phagosomal lumen into the cytosol (Dingjan et al., 2016). Since our data showed a requirement for VAMP8 in NOX2 activity, we examined whether the genetic ablation of VAMP8 would block the translocation of antigen over endosomal membranes. We used an antigen-leakage assay based on Förster resonance energy transfer (FRET) with the probe coumarin-cephalosporin-fluorescein (4)-acetoxymethyl (CCF4-AM) (Cebrian et al., 2011; Dingjan et al., 2016; Ray et al., 2010). CCF4 accumulates in the cytosol and can be cleaved by the enzyme β-lactamase, which results in a loss of FRET between its coumarin (donor) and fluorescein (acceptor) fluorophores. Mammalian cells do not produce β-lactamase, but exogenous β-lactamase can be taken up by DCs and escape from endosomes into the cytosol where it can cleave CCF4. We performed side-by-side comparisons where we first loaded VAMP8 knockdown and control DCs with CCF4 and then cultured them in the presence of exogenous

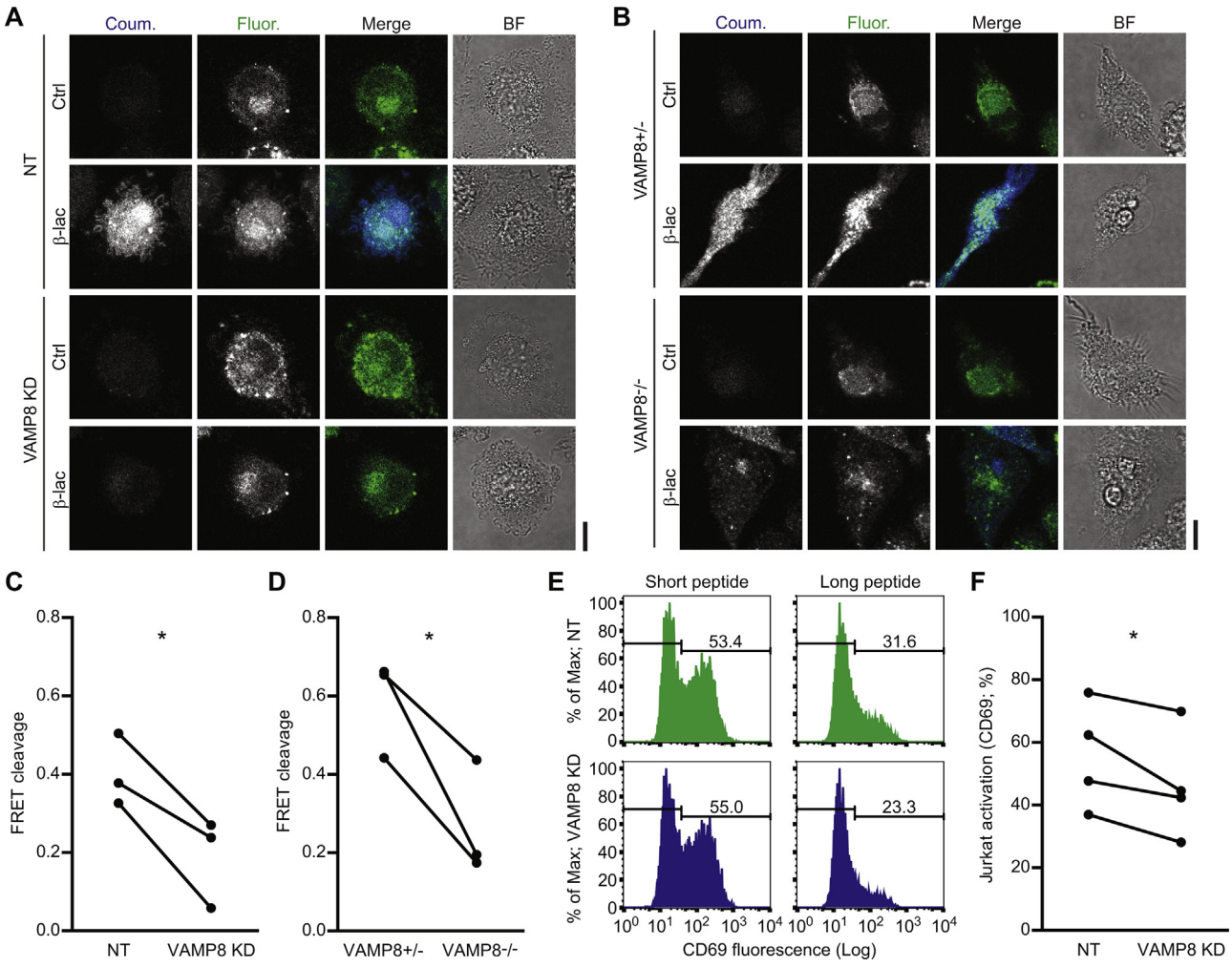

Fig. 3. Antigen cross-presentation depends on VAMP8-mediated trafficking of NOX2. (A) Representative confocal microscope images of the CCF4 endosomal leakage assay for VAMP8 siRNA knockdown (VAMP8 KD) and non-targeting siRNA (NT) human DCs. The cytosolic FRET probe CCF4 was cleaved by exogenous β-lactamase (β-lac) resulting in a decreased ratio of fluorescein (acceptor fluorophore; green in merge) over coumarin (donor; blue) fluorescence. (B) Representative confocal microscope images as in panel A, but now for VAMP8-/- and VAMP8± mouse BMDCs. (C) Quantification of panel A. The graph shows the CCF4 cleavage efficiencies (see reference (Dingjan et al., 2016)) of DCs from 3 donors (linked by solid lines; $p = 0.0312$). (D) Same as panel C, but now for VAMP8-/- and VAMP8± mouse BMDCs (panel B; $p = 0.0457$). (E) Representative flow cytometry histograms of CD69 expression by Jurkat cells carrying a gp100-specific T cell receptor. The jurkat T cells were co-cultured with VAMP8 KD (blue) and NT (green) DCs that were loaded with short (residues 280–288; left-hand graphs) or long (residues 272–300; right) gp100 peptide. The percentages CD69-positive T cells are indicated in the graphs. (F) Quantification of T cell activation from panel E for 4 donors ($p = 0.0461$). Scale bars, 10 μm. (For interpretation of the references to colour in this figure legend, the reader is referred to the web version of this article.)

β-lactamase purified from *Escherichia coli* (Fig. 3A–B). The DCs were stimulated with LPS in these experiments, although we cannot exclude additional PRR-signaling from bacterial contaminants in the β-lactamase. Compared to the control cells, CCF4 cleavage was reduced both with human DCs with siRNA knockdown of VAMP8 and with mouse VAMP8-/- BMDCs (Fig. 3C–D). Thus, the absence of VAMP8 leads to reduced antigen translocation over endosomal membranes.

The release of antigen from endosomes into the cytosol is well-known to promote antigen cross-presentation by making it accessible to degradation by the proteasome (Cruz et al., 2017; Joffre et al., 2012; Nair-Gupta and Blander, 2013). We therefore reasoned that the reduced endosomal antigen release we observed upon genetic ablation of VAMP8 could well explain known defects in antigen cross-presentation by BMDCs from VAMP8-/- mice (Matheoud et al., 2013). To further examine the potential involvement of VAMP8 in cross-presentation, we investigated whether knockdown of VAMP8 would impair antigen cross-presentation by human DCs. We cultured our human DCs with a long peptide of the melanoma antigen gp100 (residues 272–300). DCs that take up and process this peptide can cross-present a small fragment of this peptide (residues 280–288) to a Jurkat T cell line carrying a receptor specific for this fragment (Dingjan et al., 2016). We also incubated DCs with this short $gp100_{280-288}$ peptide which can be directly loaded on MHC class I and thereby allows to measure direct presentation. Jurkat T cell activation results in upregulated expression of the maturation marker CD69 on its surface. Jurkat T cell activation by VAMP8-knockdown DCs was reduced compared to the non-targeting siRNA control for the long, but not the short, peptide (Fig. 3E–F). Although this reduction was relatively small, it was significant and similar to the inhibitions that we observed previously by direct siRNA knockdown of $gp91^{phox}$ or by treatment with the proteasome inhibitors MG132 and lactacystin (Dingjan et al., 2016), which suggests that NOX2 activation is necessary for cross-presentation via the cytosolic, TAP- and proteasome-dependent pathway. The decreased T cell activation upon VAMP8 knockdown was not caused by reduced surface levels of MHC class I (Fig. 1C) because this reduction was no longer significant for matured DCs (Sup. Fig. 3) and because direct presentation of the short $gp100_{280-288}$ peptide was not affected. Together,

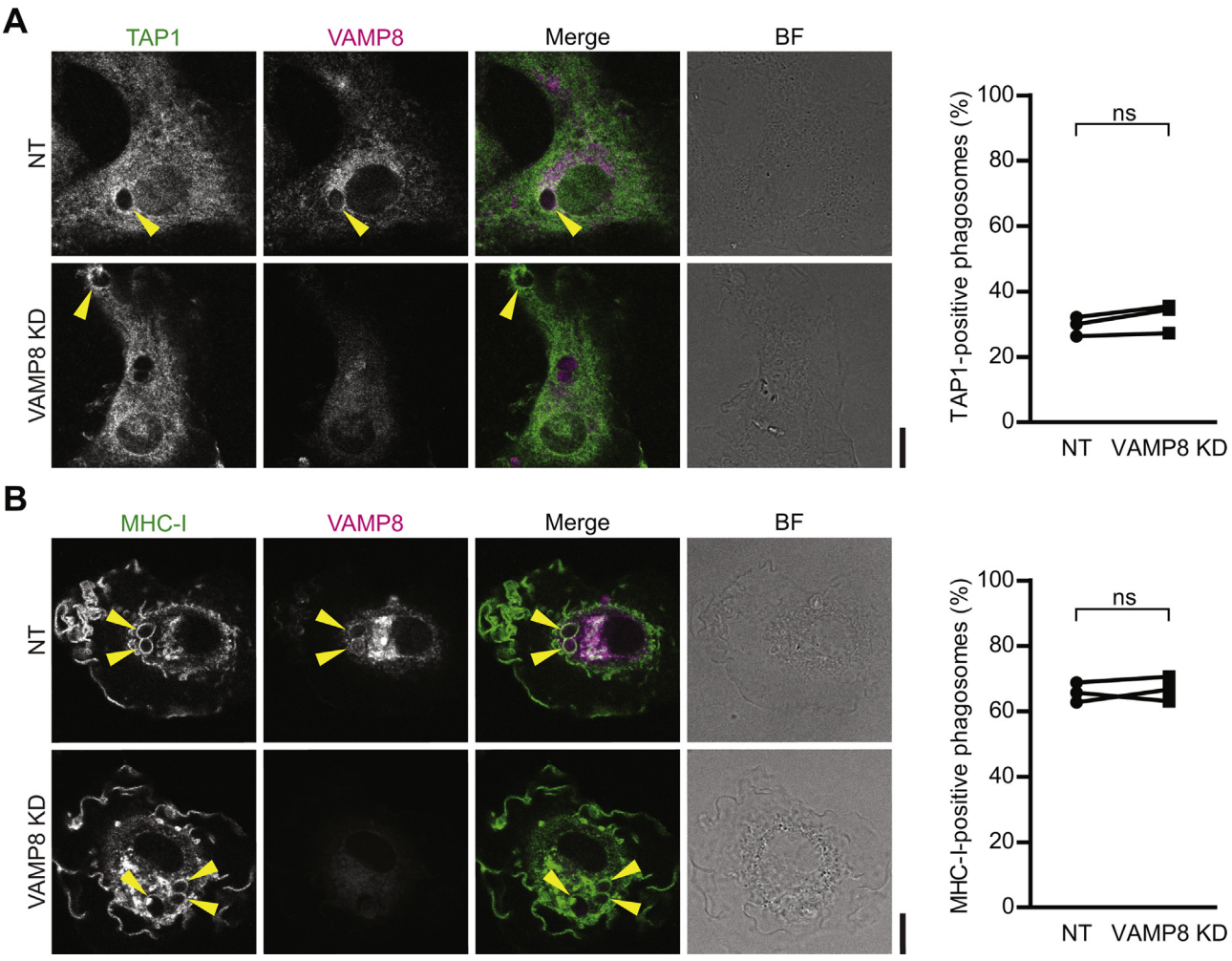

Fig. 4. Recruitment of TAP1 and MHC class I molecules to phagosomes is VAMP8-independent. (A) Representative confocal micrographs showing the recruitment of TAP1 (green in merge) and VAMP8 (magenta) to zymosan-containing phagosomes by immunofluorescence in VAMP8 KD and NT human DCs. Arrow heads indicate phagosomes positive for TAP1. The graph shows the quantification by manual counting of TAP1-positive phagosomes of DCs from 3 individual donors. (B) Same as panel A, but now for MHC class I (MHC-I; green in merge). Scale bars, 10 μm; ns: not significant. (For interpretation of the references to colour in this figure legend, the reader is referred to the web version of this article.)

these data are in accordance with a role for VAMP8 in delivery of gp91^{phox} to the antigen-containing compartment for antigen cross-presentation.

In the final set of experiments, we investigated whether the VAMP8-mediated transport of gp91^{phox} to phagosomes would also be responsible for the recruitment of other components involved in antigen cross-presentation. Antigen cross-presentation is promoted by the phagosomal presence of TAP1, an antigen transporter channel that mainly resides at the endoplasmic reticulum (ER) (Sup. Fig. 4A; Guermonprez et al., 2003). TAP1 is recruited from the ER to antigen-containing phagosomes by the action of Sec22b, another R-SNARE active at the ER-Golgi intermediate compartment (ERGIC; Sup. Fig. 4B; Cebrian et al., 2011). The phagosomal recruitment of TAP1 was not affected by knockdown of VAMP8 (Fig. 4A). Moreover, we observed only little, if any, localization of Sec22b to the phagosome and did not observe overlap between gp91^{phox} and the ER marker Calnexin (Sup. Fig. 4C–D), indicating that gp91^{phox} and TAP1 are recruited to the phagosome via different pathways.

We also tested whether VAMP8 would mediate recruitment of MHC class I to phagosomes. MHC class I molecules are recruited to phagosomes from Rab11a-positive recycling endosomal compartments (Nair-Gupta et al., 2014). This is critical for antigen cross-presentation as Rab11a-silencing reduces MHC class I recruitment and results in impaired cross-presentation (Nair-Gupta et al., 2014). MHC class I traffics to phagosomes by the action of the SNARE SNAP23 (Nair-Gupta et al., 2014), which also mediates phagosomal recruitment of gp91^{phox} together with VAMP8 (Dingjan et al., 2017). However, despite that both gp91^{phox} and MHC class I traffic to phagosomes by the action of SNAP23 (Dingjan et al., 2017; Nair-Gupta et al., 2014), VAMP8 does not seem to mediate phagosomal trafficking of the latter, because genetic ablation of VAMP8 does not affect the recruitment of MHC class I to phagosomes in mouse BMDCs (Nair-Gupta et al., 2014). This is in agreement with our findings, as siRNA knockdown of VAMP8 did not affect phagosomal recruitment of MHC class I in human DCs (Fig. 4B), even though part of gp91^{phox} located at Rab11a-positive recycling endosomal compartments and phagosomes (Sup. Fig. 4E). Overall, our results and published data (Cebrian et al., 2011; Nair-Gupta et al., 2014) argue for the independent trafficking of gp91^{phox}, MHC class I and TAP1 to the antigen-containing compartment, with each of these proteins facilitating the processing of the antigen for cross-presentation.

4. Discussion

This study is an extension of two previous studies where we showed (i) that NOX2-produced ROS induce antigen translocation from endosomes into the cytosol promoting antigen

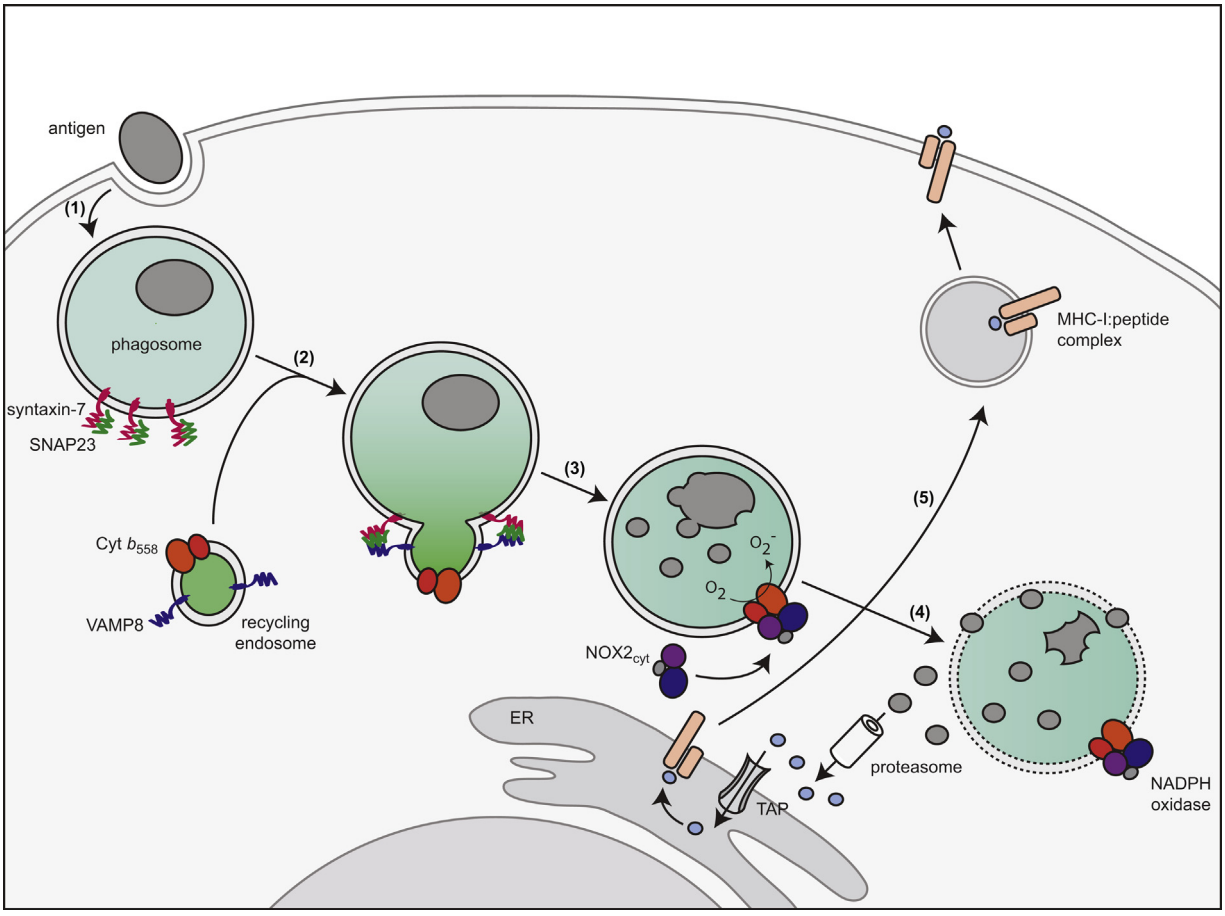

Fig. 5. Model of VAMP8-mediated antigen cross-presentation. (step 1) Uptake of antigen via endocytosis or phagocytosis. (2) Recruitment of cytochrome b_{558} (Cyt b_{558}) to the antigen-containing compartment by VAMP8, SNAP23 and syntaxin-7. (3) The cytosolic subunits of NOX2 ($NOX2_{cyt}$; consisting of $p40^{phox}$, $p47^{phox}$ and $p67^{phox}$) and the small GTPase Rac are recruited to cytochrome b_{558}. Fully assembled NOX2 on the phagosome produces ROS in the organellar lumen. (4) ROS lead to disruption of the phagosomal membrane allowing translocation of antigen into the cytosol. In the cytosol, the antigen becomes accessible for degradation by the proteasome. The proteasome-derived peptide fragments are imported in the endoplasmatic reticulum (ER) by the transporter associated with antigen processing (TAP) for loading onto MHC class I molecules (MHC-I). (5) The MHC:peptide complex is transported to the cell surface to cross-present the antigen to naive cytolytic T cells.

cross-presentation (Dingjan et al., 2016) and (ii) that phagosomal recruitment of the integral membrane component of NOX2 is mediated by the SNARE protein VAMP8 (Dingjan et al., 2017). This study is also an extension of a recent study by Matheoud et al. (Matheoud et al., 2013) who showed that $gp91^{phox}$ recruitment to phagosomes is inhibited in the absence of VAMP8 and that this leads to alkalization of the phagosomal lumen, decreased proteolysis and defects in antigen cross-presentation. In this study, we show that genetic ablation of VAMP8 in both human and mouse DCs not only impairs NOX2 recruitment to the antigen-containing compartment, but also prevents auto-oxidation of endosomal membranes and blocks endosomal antigen release into the cytosol. Our data support the previously observed role for VAMP8 in antigen cross-presentation in mouse DCs (Matheoud et al., 2013), as we show that siRNA knockdown of VAMP8 leads to impaired antigen cross-presentation in human DCs.

VAMP8-mediated trafficking of NOX2 to phagosomes seems independent from the phagosomal recruitment of TAP1 and MHC class I, two other protein complexes required for antigen cross-presentation. We found that whereas VAMP8 knockdown resulted in reduced recruitment of $gp91^{phox}$ to phagosomes, the phagosomal presence of TAP1 and MHC class I were not affected. This finding data is in line with literature: Nair-Gupta et al. showed that MHC class I is recruited to phagosomes from Rab11a-positive recycling endosomes and this recruitment is not affected in DCs from VAMP8-knockout mice (Nair-Gupta et al., 2014). Cebrian et al. showed that TAP1 is recruited to phagosomes from the ER-Golgi intermediate compartment by the action of Sec22b, another R-SNARE (Cebrian et al., 2011). In contrast, our data and literature (Dingjan et al., 2017; Matheoud et al., 2013) show that $gp91^{phox}$ is recruited to phagosomes from compartments of lysosomal nature by the action of VAMP8. Thus, it is becoming increasingly clear that NOX2 traffics to phagosomes independent of TAP1 and MHC class I. NOX2 has a role early in cross-presentation and promotes the translocation of antigen into the cytosol and reduces activation of endo/lysosomal proteases by increased pH and/or reversible oxidation (Allan et al., 2014; Dingjan et al., 2016; Jancic et al., 2007; Kotsias et al., 2013; Rybicka et al., 2012; Savina et al., 2006). In addition, NOX2 mediates the killing of ingested microbes by DCs (Vulcano et al., 2004). TAP1 and MHC class I play roles later during cross-presentation as they mediate antigen transport, loading and presentation (Cruz et al., 2017; Joffre et al., 2012; Nair-Gupta and Blander, 2013). The independent trafficking of NOX2 to antigen-containing compartments might allow to uncouple ROS production from these later functions and thereby could allow better spatial and/or temporal control of antigen processing and presentation.

The defects we observed in endosomal antigen release and cross-presentation upon genetic ablation of VAMP8 are relatively mild. This is likely caused by the fact that not all $gp91^{phox}$ traffics to the antigen containing compartment by the action of VAMP8, but that part of $gp91^{phox}$ reaches the phagosome from the plasma membrane during antigen internalization (Dingjan et al., 2017).

Another likely explanation for the relatively small effects of VAMP8 knockdown/knockout is that SNARE proteins are redundant and promiscuous and other SNARE proteins may at least partially compensate for the absence of VAMP8. Indeed, in many studies the knockdown or knockout of SNARE proteins did not result in clear changes in phenotype (Bethani et al., 2009; Hong, 2005; Nair-Gupta et al., 2014). Moreover, we found relatively mild phenotypes of a ~25% reduction of surface expressed MHC class I and a trend towards lower IL-1ra secretion upon VAMP8 knockdown in human DCs. A key candidate for such a compensatory role is VAMP3, which locates to endosomes and phagosomes similar to VAMP8 (Matheoud et al., 2013; Nair-Gupta et al., 2014; Verboogen et al., 2017). The observed differences in antigen presentation might also be relatively small, because the absence of VAMP8 does not influence phagosomal recruitment of MHC class I and TAP1 and part of the cross-presentation machinery remains intact.

Our data support the following model of how VAMP8 promotes antigen cross-presentation by DCs (Fig. 5). First, foreign antigen is ingested by the DCs. Second, gp91^{phox} traffics to the antigen-containing compartment by the concerted action of VAMP8, SNAP23 and syntaxin-7 (Dingjan et al., 2017). Third, NOX2 assembles on the antigen-containing compartment and produces ROS in the organellar lumen. These ROS lead to an increase of the luminal pH as well as to auto-oxidation of endo/lysosomal proteases and of the endo/phagosomal membranes. Fourth, the auto-oxidation disrupts the membrane integrity, allowing the translocation of antigen into the cytosol, where it becomes accessible to proteasomal degradation. In the final step, the proteasome-derived peptide fragments can either be re-imported into the endosomes/phagosomes or be imported in the endoplasmatic reticulum by the transporter associated with antigen processing (TAP) for loading onto MHC class I molecules (Cruz et al., 2017; Joffre et al., 2012; Nair-Gupta and Blander, 2013). In addition to the SNARE molecules VAMP8, SNAP23 and syntaxin-7 (Dingjan et al., 2017), previous studies have identified several key molecules for regulating the delivery of gp91^{phox} to the antigen-containing compartment. One of these molecules is synaptotagmin 11 which mediates the delivery of gp91^{phox} to phagosomes in RAW264.7 macrophages (Arango Duque et al., 2013). Another key protein is the small GTPase Rab27a which is necessary for efficient recruitment of gp91^{phox} to phagosomes in mouse BMDCs (Jancic et al., 2007). Our data show that both these proteins are expressed in human DCs (not shown) and it seems likely that these proteins regulate the delivery of gp91^{phox} to the antigen containing compartment also in these cells. If and by which mechanism synaptotagmin 11 and Rab27a regulate the SNARE complexing of VAMP8 with SNAP23 and sytaxin-7 remains to be elucidated. Overall, our results strengthen the emerging concept that the intracellular trafficking of the integral component of NOX2 to phagosomes is a key regulatory mechanism for antigen cross-presentation.

Author contributions

ID, MtB and GvdB designed experiments; ID, DRJV and LP performed experiments; GFM contributed to VAMP8-/- experiments; ID analyzed data; ID and GvdB wrote the manuscript.

Acknowledgements

GvdB is funded by a Hypatia fellowship from the Radboud University Medical Center and is the recipient of a Career Development Award from the Human Frontier Science Program, a Starting Grant from the European Research Council (ERC) under the European Union's Seventh Framework Programme (Grant Agreement Number 336479) and a grant from the Netherlands Organization for Scientific Research (NWO-ALW VIDI 864.14.001). This work was supported by the NWO Gravitation Programme 2013 (ICI-024.002.009).

Appendix A. Supplementary data

Supplementary data associated with this article can be found, in the online version, at **http://dx.doi.org/10.1016/j.ejcb.2017.06.007**.

References

Allan, E.R.O., Tailor, P., Balce, D.R., Pirzadeh, P., McKenna, N.T., Renaux, B., Warren, A.L., Jirik, F.R., Yates, R.M., 2014. NADPH oxidase modifies patterns of MHC class II-restricted epitopic repertoires through redox control of antigen processing. J. Immunol. 192, 4989–5001, http://dx.doi.org/10.4049/jimmunol.1302896.

Antonin, W., Holroyd, C., Tikkanen, R., Höning, S., Jahn, R., 2000. The R-SNARE endobrevin/VAMP-8 mediates homotypic fusion of early endosomes and late endosomes. Mol. Biol. Cell 11, 3289–3298, http://dx.doi.org/10.1091/mbc.11.10.3289.

Arango Duque, G., Fukuda, M., Descoteaux, A., 2013. Synaptotagmin XI regulates phagocytosis and cytokine secretion in macrophages. J. Immunol. 190, 1737–1745, http://dx.doi.org/10.4049/jimmunol.1202500.

Baranov, M.V., Ter Beest, M., Reinieren-Beeren, I., Cambi, A., Figdor, C.G., van den Bogaart, G., 2014. Podosomes of dendritic cells facilitate antigen sampling. J. Cell Sci. 127, 1052–1064, http://dx.doi.org/10.1242/jcs.141226.

Baranov, M.V., Revelo, N.H., Dingjan, I., Maraspini, R., Ter Beest, M., Honigmann, A., van den Bogaart, G., 2016. SWAP70 organizes the actin cytoskeleton and is essential for phagocytosis. Cell Rep. 17, 1518–1531, http://dx.doi.org/10.1016/j.celrep.2016.10.021.

Bethani, I., Werner, A., Kadian, C., Geumann, U., Jahn, R., Rizzoli, S.O., 2009. Endosomal fusion upon SNARE knockdown is maintained by residual snare activity and enhanced docking. Traffic 10, 1543–1559, http://dx.doi.org/10.1111/j.1600-0854.2009.00959.x.

Cebrian, I., Visentin, G., Blanchard, N., Jouve, M., Bobard, A., Moita, C., Enninga, J., Moita, L.F., Amigorena, S., Savina, A., 2011. Sec22b regulates phagosomal maturation and antigen crosspresentation by dendritic cells. Cell 147, 1355–1368, http://dx.doi.org/10.1016/j.cell.2011.11.021.

Choudhury, A., Dominguez, M., Puri, V., Sharma, D.K., Narita, K., Wheatley, C.L., Marks, D.L., Pagano, R.E., 2002. Rab proteins mediate Golgi transport of caveola-internalized glycosphingolipids and correct lipid trafficking in Niemann-Pick C cells. J. Clin. Invest. 109, 1541–1550, http://dx.doi.org/10.1172/JCI15420.

Cruz, F.M., Colbert, J.D., Merino, E., Kriegsman, B.A., Rock, K.L., 2017. The biology and underlying mechanisms of cross-presentation of exogenous antigens on MHC-I molecules. Annu. Rev. Immunol., 149–176, http://dx.doi.org/10.1146/annurev-immunol-041015-055254.

Dingjan, I., Verboogen, D.R., Paardekooper, L.M., Revelo, N.H., Sittig, S.P., Visser, L.J., Mollard, G.F., von Henriet, S.S., Figdor, C.G., Ter Beest, M., van den Bogaart, G., 2016. Lipid peroxidation causes endosomal antigen release for cross-presentation. Sci. Rep. 6, 22064, http://dx.doi.org/10.1038/srep22064.

Dingjan, I., Linders, P.T.A., van den Bekerom, L., Baranov, M.V., Halder, P., Ter Beest, M., van den Bogaart, G., 2017. Oxidized phagosomal NOX2 complex is replenished from lysosomes. J. Cell Sci. 130, 1285–1298, http://dx.doi.org/10.1242/jcs.196931.

Dressel, R., Elsner, L., Novota, P., Kanwar, N., Fischer von Mollard, G., 2010. The exocytosis of lytic granules is impaired in Vti1b- or Vamp8-deficient CTL leading to a reduced cytotoxic activity following antigen-specific activation. J. Immunol. 185, 1005–1014, http://dx.doi.org/10.4049/jimmunol.1000770.

Guermonprez, P., Saveanu, L., Kleijmeer, M., Davoust, J., Van Endert, P., Amigorena, S., 2003. ER-phagosome fusion defines an MHC class I cross-presentation compartment in dendritic cells. Nature 425, 397–402, http://dx.doi.org/10.1038/nature01911.

Hari, A., Ganguly, A., Mu, L., Davis, S.P., Stenner, M.D., Lam, R., Munro, F., Namet, I., Alghamdi, E., Fürstenhaupt, T., Dong, W., Detampel, P., Shen, L.J., Amrein, M.W., Yates, R.M., Shi, Y., 2015. Redirecting soluble antigen for MHC class I cross-presentation during phagocytosis. Eur. J. Immunol. 45, 383–395, http://dx.doi.org/10.1002/eji.201445156.

Ho, Y.H.S., Cai, D.T., Wang, C.-C., Huang, D., Wong, S.H., 2008. Vesicle-associated membrane protein-8/endobrevin negatively regulates phagocytosis of bacteria in dendritic cells. J. Immunol. 180, 3148–3157, http://dx.doi.org/10.4049/jimmunol.180.5.3148.

Ho, Y.H.S., Cai, D.T., Huang, D., Wang, C.C., Wong, S.H., 2009. Caspases regulate VAMP-8 expression and phagocytosis in dendritic cells. Biochem. Biophys. Res. Commun. 387, 371–375, http://dx.doi.org/10.1016/j.bbrc.2009.07.028.

Hong, W., 2005. SNAREs and traffic. Biochim. Biophys. Acta 1744, 120–144, http://dx.doi.org/10.1016/j.bbamcr.2005.03.014.

Jancic, C., Savina, A., Wasmeier, C., Tolmachova, T., El-Benna, J., Dang, P.M.-C., Pascolo, S., Gougerot-Pocidalo, M.-A., Raposo, G., Seabra, M.C., Amigorena, S., 2007. Rab27a regulates phagosomal pH and NADPH oxidase recruitment to dendritic cell phagosomes. Nat. Cell Biol. 9, 367–378, http://dx.doi.org/10.1038/ncb1552.

Joffre, O.P., Segura, E., Savina, A., Amigorena, S., 2012. Cross-presentation by dendritic cells. Nat. Rev. Immunol. 12, 557–569, http://dx.doi.org/10.1038/nri3254.

Kanwar, N., Fayyazi, A., Backofen, B., Nitsche, M., Dressel, R., von Mollard, G.F., 2008. Thymic alterations in mice deficient for the SNARE protein VAMP8/endobrevin. Cell Tissue Res. 334, 227–242, http://dx.doi.org/10.1007/s00441-008-0692-7.

Kotsias, F., Hoffmann, E., Amigorena, S., Savina, A., 2013. Reactive oxygen species production in the phagosome: impact on antigen presentation in dendritic cells. Antioxid. Redox Signal. 18, 714–729, http://dx.doi.org/10.1089/ars.2012.4557.

Mantegazza, A.R., Savina, A., Vermeulen, M., Pérez, L., Geffner, J., Hermine, O., Rosenzweig, S.D., Faure, F., Amigorena, S., 2008. NADPH oxidase controls phagosomal pH and antigen cross-presentation in human dendritic cells. Blood 112, 4712–4722, http://dx.doi.org/10.1182/blood-2008-01-134791.

Matheoud, D., Moradin, N., Bellemare-Pelletier, A., Shio, M.T., Hong, W.J., Olivier, M., Gagnon, E., Desjardins, M., Descoteaux, A., 2013. Leishmania evades host immunity by inhibiting antigen cross-presentation through direct cleavage of the SNARE VAMP8. Cell Host Microbe 14, 15–25, http://dx.doi.org/10.1016/j.chom.2013.06.003.

Nagamatsu, S., Nakamichi, Y., Watanabe, T., Matsushima, S., Yamaguchi, S., Ni, J., Itagaki, E., Ishida, H., 2001. Localization of cellubrevin-related peptide, endobrevin, in the early endosome in pancreatic beta cells and its physiological function in exo-endocytosis of secretory granules. J. Cell Sci. 114, 219–227.

Nair-Gupta, P., Blander, J.M., 2013. An updated view of the intracellular mechanisms regulating cross-presentation. Front. Immunol. 4, 401, http://dx.doi.org/10.3389/fimmu.2013.00401.

Nair-Gupta, P., Baccarini, A., Tung, N., Seyffer, F., Florey, O., Huang, Y., Banerjee, M., Overholtzer, M., Roche, P. a., Tampé, R., Brown, B.D., Amsen, D., Whiteheart, S.W., Blander, J.M., 2014. TLR signals induce phagosomal MHC-I delivery from the endosomal recycling compartment to allow cross-presentation. Cell 158, 506–521, http://dx.doi.org/10.1016/j.cell.2014.04.054.

Nunes, P., Demaurex, N., Dinauer, M.C., 2013. Regulation of the NADPH oxidase and associated ion fluxes during phagocytosis. Traffic 14, 1118–1131, http://dx.doi.org/10.1111/tra.12115.

Paumet, F., Le Mao, J., Martin, S., Galli, T., David, B., Blank, U., Roa, M., 2000. Soluble NSF attachment protein receptors (SNAREs) in RBL-2H3 mast cells: functional role of syntaxin 4 in exocytosis and identification of a vesicle-associated membrane protein 8-containing secretory compartment. J. Immunol. 164, 5850–5857, http://dx.doi.org/10.4049/jimmunol.164.11.5850.

Polgár, J., Chung, S.-H., Reed, G.L., 2002. Vesicle-associated membrane protein 3 (VAMP-3) and VAMP-8 are present in human platelets and are required for granule secretion. Blood 100, 1081–1083, http://dx.doi.org/10.1182/blood.V100.3.1081.

Pryor, P.R., Mullock, B.M., Bright, N.a., Lindsay, M.R., Gray, S.R., Richardson, S.C.W., Stewart, A., James, D.E., Piper, R.C., Luzio, J.P., 2004. Combinatorial SNARE complexes with VAMP7 or VAMP8 define different late endocytic fusion events. EMBO Rep. 5, 590–595, http://dx.doi.org/10.1038/sj.embor.7400150.

Ray, K., Bobard, A., Danckaert, A., Paz-Haftel, I., Clair, C., Ehsani, S., Tang, C., Sansonetti, P., Tran, G.V.N., Enninga, J., 2010. Tracking the dynamic interplay between bacterial and host factors during pathogen-induced vacuole rupture in real time. Cell. Microbiol. 12, 545–556, http://dx.doi.org/10.1111/j.1462-5822.2010.01428.x.

Rybicka, J.M., Balce, D.R., Chaudhuri, S., Allan, E.R.O., Yates, R.M., 2012. Phagosomal proteolysis in dendritic cells is modulated by NADPH oxidase in a pH-independent manner. EMBO J. 31, 932–944, http://dx.doi.org/10.1038/emboj.2011.440.

Savina, A., Jancic, C., Hugues, S., Guermonprez, P., Vargas, P., Moura, I.C., Lennon-Duménil, A.-M., Seabra, M.C., Raposo, G., Amigorena, S., 2006. NOX2 controls phagosomal pH to regulate antigen processing during crosspresentation by dendritic cells. Cell 126, 205–218, http://dx.doi.org/10.1016/j.cell.2006.05.035.

Verboogen, D.R.J., González Mancha, N., Ter Beest, M., van den Bogaart, G., 2017. Fluorescence lifetime imaging microscopy reveals rerouting of SNARE trafficking driving dendritic cell activation. Elife 6, http://dx.doi.org/10.7554/elife.23525.

Vulcano, M., Dusi, S., Lissandrini, D., Badolato, R., Mazzi, P., Riboldi, E., Borroni, E., Calleri, A., Donini, M., Plebani, A., Notarangelo, L., Musso, T., Sozzani, S., 2004. Toll receptor-mediated regulation of NADPH oxidase in human dendritic cells. J. Immunol. 173, 5749–5756, http://dx.doi.org/10.4049/jimmunol.173.9.5749.

Wagner, C.S., Cresswell, P., 2012. TLR and nucleotide-binding oligomerization domain-like receptor signals differentially regulate exogenous antigen presentation. J. Immunol. 188, 686–693, http://dx.doi.org/10.4049/jimmunol.1102214.